The 2009 IEEE/RSJ International Conference on
Intelligent Robots and Systems
October 11-15, 2009 St. Louis, USA

Characterization of Vertically Aligned Carbon Nanofibers Grown on Ni Dots Nanoelectrode Array Using Atomic Force Microscopy

Zhuxin Dong, *Student Member, IEEE*, Uchechukwu C. Wejinya, *Member, IEEE*, Imad H. Elhajj, *Senior Member, IEEE*, and Meyya Meyyappan, *Fellow, IEEE*

Abstract—One of the major limitations in the development of ultrasensitive electrochemical biosensors based on one-dimensional nanostructure is the difficulty involved with reliably fabricating nanoelectrode arrays (NEAs). In previous work, a simple, robust and scalable wafer-scale fabrication method to produce multiplexed biosensors is introduced. Each sensor chip consists of nine individually addressable arrays that uses electron beam patterned vertically aligned carbon nanofibers (VACNFs) as the sensing element. To ensure nanoelectrode behavior with higher sensitivity, VACNFs were precisely grown on 100 nm Ni dots with 1μm spacing on each micro pad. However, in order to examine the quality and measure the height and diameter of the VACNFs, some surface detection and measurement tool at the nanoscale level is needed. In this paper, we introduce an approach to measure these nano-scale features through Atomic Force Microscope (AFM). With this method, both the 2D and 3D images of sample surface are generated and the sizes of carbon nanofibers and cavities are obtained. Furthermore, statistical analysis is carried out to enable improvement of VACNFs growth and fabrication.

I. Introduction

With the recent increase in pathogen outbreaks in water, food and other media, new methods and technologies for detection and quantification are needed. These devices and systems will need to be fast, reliable, ultrasensitive, portable, and automated. For several decades, detection heavily relied on an indicator organism approach to assess the microbiological quality of drinking water. But an increased understanding of the diversity of waterborne pathogens has concluded that the use of bacterial indicators may not be as universally protective as was once thought [1]. Newer methods involving immunofluorescence techniques and nucleic acid analysis provide valuable opportunities for rapid and more specific analytical methods. Particularly, electrochemical (EC) biosensors are attractive for detecting a wide range of species, including proteins, nucleic acids, small molecules and viruses because of their relative simplicity, portability, low cost and low power requirement. EC biosensors consist of two primary components: a recognition layer containing a biomolecule and an electrochemical signal transducer. They make use of electrochemical reactions or the surface property changes upon target binding. Advances in microfabrication technology have provided electrode configurations such as microelectrode arrays [2] and interdigitated arrays (IDA) [3], but their performance can be further enhanced by miniaturizing to nanoscale. Recent progress in nanofabrication technologies like electron beam lithography and nanoimprinting enable fabrication of one-dimensional nanostructure electrodes, like carbon nanofibers [4][5][6], carbon nanotube bundles [7][8], nanoscale IDA [9], silicon nanowires [10] and diamond nanowires [11], which are capable of high spatial and temporal resolutions, possibly yielding sufficient sensitivity to single molecule detection. Among various types of one-dimensional nanoscale electrodes, vertically aligned carbon nanofibers (VACNFs) have received tremendous attention because of their attractive properties such as high electrical and thermal conductivities, superior mechanical strength, a wide electrochemical potential window, flexible surface chemistry and biocompatibility [12][13]. Compared to other carbon materials such as glassy carbon, carbon black, carbon microfibers, and pyrolytic graphite, the open-ended VACNF arrays present well-defined edgeplane structure suitable for selective covalent functionalization of primary amine-terminated oligonucleotide probes. Thus, the micro chip, a 3×3 array biosensor using nanopatterned VACNF array for detection of chemical particles, such as *E. coli* O157:H7, has been achieved [14]. However, to examine how well the growth of VACNFs is, an advanced tool such as AFM is employed.

Atomic Force Microscope (AFM) is a very high-resolution type of scanning probe microscope that has resolution of fractions of a nanometer. The AFM was created specifically to generate a three-dimensional view of a scanned object, unlike the Scanning Electron Microscope (SEM) that can only produce two dimensional views. With the ability to scan almost any type of surface, the AFM is used in many types of research. Surfaces include polymers, ceramics, composites, glass, and biological samples. The

Zhuxin Dong is Ph.D. Candidate with the Department of Mechanical Engineering, University of Arkansas, Fayetteville, AR 72701 USA (corresponding author to provide phone: 479-575-6821; fax: 479-575-6982; e-mail: dzhuxin@uark.edu).

Uchechukwu C. Wejinya is an Assistant Professor with the Mechanical Engineering Department, University of Arkansas, Fayetteville, AR 72701 USA (e-mail: uwejinya@uark.edu).

Imad H. Elhajj is with the Department of Electrical and Computer Engineering, American University of Beirut, Beirut, Lebanon (e-mail: ie05@aub.edu.lb).

Meyya Meyyappan is the Director and Senior Scientist at Ames' Center for Nanotechnology, Moffett Field, CA 94035 USA (e-mail: m.meyyappan@nasa.gov).

AFM also has a variety of operation modes including contact mode, lateral force microscopy, noncontact mode, tapping mode, and phase imaging. This feature induces the stunning capabilities of this microscope by only applying a simple set of modifications. The microscope uses a micro scale cantilever with a probe at the end that is used to scan a surface. A beam deflection system consisting of a laser and photodetector is built into the microscope to measure the position of the beam and ultimately the position of the cantilever tip. To calculate the force, Hooke's Law, $F = -kz$ where F is the force, k is the spring constant of the cantilever, and z is the displacement of the cantilever, is used. The laser beam is placed on the cantilever tip and the beam deflection measures the displacement the sample exerts on the cantilever. The spring constant is known based on what type of scanning probe is used. With its three dimensional capabilities and ability to operate in air rather than a vacuum sealed environment, the Atomic Force Microscope aids many studies in biological macromolecules, tribiology, optical and imaging sciences. The microscope has the capabilities of scanning living organisms through the study of measurements of protein-ligand interactions on living cells and many other research applications. The atomic force microscope has been used as the primary microscope in the direct measurement of interatomic force gradients, detection and localization of single molecular recognition events, single molecule experiments at the solid-liquid interface and fractured polymer/silica fiber surface research. Owing to the advantages stated above, AFM is capable enough to complete the size measurement of the nano fibers and cavities.

II. Fabrication of Nanoelectrode VACNFs

The intensively sensitive fabrication process of VACNF NEAs includes six major steps done on a four inch silicon (100) wafer that was previously coated with 500 nm of silicon dioxide. The steps of the fabrication process as well as the corresponding SEM images are shown in Figure 1 and Figure 2, respectively. The steps include A) metal deposition for micro pads, contact pads and electrical interconnects; (B) nanopatterning of Ni catalyst dots; (C) directional growth of CNFs; (D) silicon dioxide deposition for electrical isolation and mechanical support; (E) chemical mechanical polishing (CMP) to expose CNF tips, and (F) a wet etch with 7:1 HF to expose contact pads.

A. Deposition of Metal

Using optical lithography patterning, 30 chips are able to be patterned onto the four inch wafer. Each chip contains nine contact pads that are attached by electrical-interconnects to a single 3×3 set of arrays. Each of the nine arrays measure 200 microns square and the contact pads measure two centimeters square. Electrically, the underlying oxide isolates the pads. Using a one micron thick Shipley -

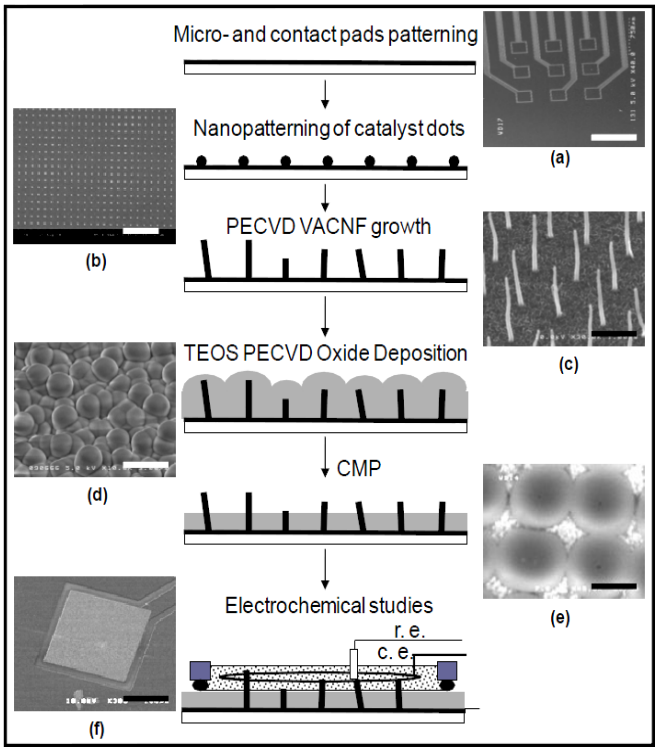

Fig. 1. The procedure of fabricating biosensors based on nanopatterned VACNFs: (a) deposition of metal; (b) nanopatterning; (c) growth of CNFs; (d) deposition of silicon dioxide; (e) chemical mechanical polishing; (f) electrochemical characterization.

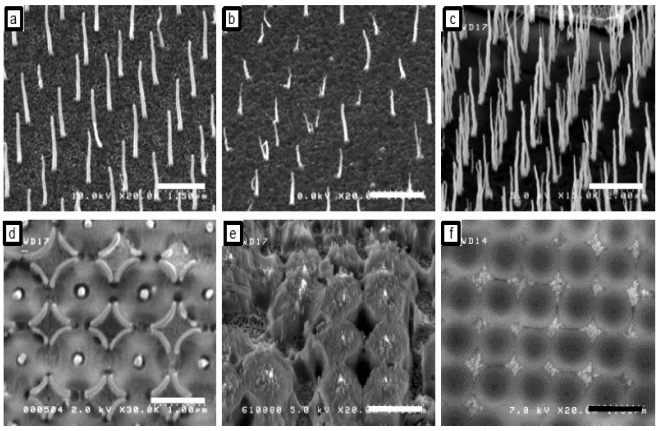

Fig. 2. Top row shows the importance of PECVD chamber conditioning on CNF growth: (a) final run in "warm chamber"; (b) initial run in "cold chamber"; (c) Effect of high thermal ramps (~200°C/min) resulting in multiple fibers from single nanopot. Bottom row illustrates SEM images of patterned arrays after re-exposing VACNF tips by Reactive Ion Etching (d), (e) and CMP (f). The dots are 100nm in diameter and 1μm in spacing.

- 3612 resist and microlithography, the pads and interconnects are patterned. An inspection under a microscope is made and then the patterns were metalized using a liftoff technique. The process of electron beam evaporation is then used to deposit a 200 nm thick Cr film and then the wafer is immersed in acetone for one hour. Once removed from the acetone, the wafer is sprayed with methanol and isopropyl alcohol and blown dry with N_2.

B. Nanopatterning

Catalyst dots are then added to the wafer via a process

called electron beam lithography patterning. There are approximately 39,000 catalyst dots that measure 100 nm in diameter on each micropad. The process begins with spinning a 400 nm thick layer of poly methyl methacrylate onto the wafer and then baking it at 180 degrees Celsius for 90 seconds and then exposed at 100 keV, 2 nA, 1950 μC/cm2. Then immersing the exposures into a solution of half methyl isobutyl ketone and half IPA for two minutes, and then IPA for thirty seconds, the exposures are developed. The wafer was then blown dry with N_2 and examined under a microscope and again the pattern is metalized using a liftoff technique. The process of electron beam evaporation was then used to deposit a 10 nm thick film of Cr trailing with a 30 nm thick layer of Ni catalyst. The wafer was then submerged in acetone for one hour. After the time elapsed, the wafer was removed and sprayed with IPA and N_2 to blow dry.

C. Growth of CNFs

The next step is growing the VACNFs on the nickel dots that were created in step B. The growth is DC-biased PECVD growth. At a processing pressure of 6.3 mbar, plasma power of 180W and 700 degrees Celsius, 125 sccm C2H2 feedstock and 444 sccm NH3 diluent were initiated. Then a five minute thermal annealing at 600 degrees Celsius is carried out following with 250 sccm NH3. To attain the growth temperatures and thermal anneal needed, a 60 degree Celsius per minute incline was used. Each individual CNF vertically arranged to freestand on the surface with Ni catalyst on each tip. To check and affirm the process was done correctly, a fifteen minute deposition was conducted. Average results included a height of 1.5 microns, 100 nanometer base diameter, and 70 nanometer tip diameter. The uniformity of the growth was then checked by SEM.

D. Deposition of Silicon Dioxide

PECVD of silicon dioxide is managed next. To passivate the sidewalls of each individual fiber, a 3 micron SiO_2 layer was deposited onto the wafers using a pressure of 3 Torr, temperature of 400 degrees Celsius and RF power of 1000 W. The process included a parallel plate, dual RF, PECVD using a mixture of 6000 sccm of O2 and 2-3 ml/min of tetraethlyorthosilicate (TEOS). A highly conformal coating of SiO_2 was created on the newly created fibers and interconnects.

E. Chemical Mechanical Polishing

By CMP, existing of stock removal and final polish, the overrun oxide and a portion of the VACNF's are removed. This process involved removing the existing material with 0.5 m alumina (pH 4) at 10 ml/min, 60-rpm platen, 15-rpm carrier, and 15 psig down force at 150nm/min. A 0.1_m alumina (pH 4) at 10 ml/min, 60-rpm platen, 15-rpm carrier, and 25 psig down force was operated for final polish at 20nm/min. The wafer was cleaned by immersing it into a solution composed of water, hydrogen peroxide, and ammonium hydroxide at a ratio of 80:2:1 respectively and then spin-dried. The aim to re-expose the VACNF tips was carried out as well as planarization of the surface.

F. Wet Etch

To expose the contact pads, a careful etching using silicon dioxide is achieved. Optical lithography, using 2.5 micron thick Shipley resist, is again used to remove SiO_2 from the contact pads for electrical connections to the potentiostat. The Shipley resist was baked at 125 degrees Celsius for 120 seconds and immediately immersed in Shipley EC11 to be exposed and developed. The wafer was then rinsed using DI water and inspected via a microscope. Then to set the resist, the wafer was baked at 125 degrees Celsius for 180 seconds. Then using diluted HF solution, the oxide was carefully etched off of the contact pads at approximately 15 Angstroms per second. For 15 minutes, the resist was then stripped off of the wafer using EKC 830 resist stripper. The wafer was then rinsed with DI water, blown dry with N_2 and diced into 30 individual chips sized approximately 14 mm square.

III. Experimental Setup

In order to accurately determine the height and diameter of the VACNFs grown on 100nm Ni dots, an Atomic Force Microscope is employed. The AFM used in the experiment is the Agilent 5500-ILM highly sensitive microscope shown in Fig.ure 3. Figure 3 shows the experimental setup: the scan target is a single chip which contains 1×9 contact pads and a 3×3 set of nanoelectrode arrays. Each of these arrays has a 200μm square area. The scanning will be done under Acoustic AC (tapping) imaging mode and the AFM probe has a resonant frequency of 190kHz and a spring constant of 48N/m. It is important to note that the VACNFs are not electrochemically treated.

IV. Experimental Result

A. Scanning and Measurement

Before measuring the size of VACNFs and cavities their location should be found out. Thus, we scan the arrays from a 9×9μm square area in the middle. After locating the fibers and cavities in such an area, we can zoom into a 2μm square area, which encloses the identified fiber tips and cavities, to obtain clear scan image and guarantee a better and more accurate measurement. When a fiber or cavity appears clear in a scan topography image, a straight line can be drawn in any direction in the 2-Dimensinal topography image to cross the target. At the same time, we can obtain the vertical information along the line to complete a measurement. Repeat this procedure until plenty of information is available and turn to another array. Take array 1 for instance: Figure 4 illustrates a topography scan in a 9×9μm area of the array. As we can see, under such a scale only cavities are obvious. But that is enough as we can zoom in to find fiber tips surrounding the cavities. Figure 5 shows a zoomed-in -

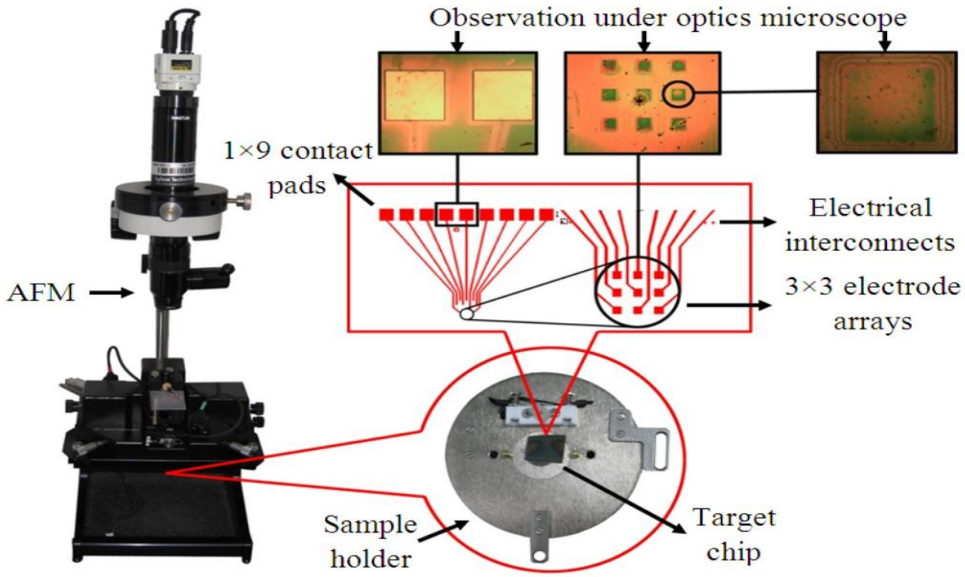

Fig. 3. Experimental setup for scanning and measurement based on AFM.

- topography in 2µm square area and besides a single cavity, there are four fiber tips in white surrounding that cavity. For a better view, a 3D image of this topography scan is generated as shown in Figure 6. The cavities are caused by the chemical TEOS, which is applied in PECVD oxide deposition. Thus, the measurement can be done by drawing lines crossing the cavity and fiber tips. Figure 7 indicates how to obtain the height and diameter of a fiber tip and the depth and diameter of a cavity from a cross-section image.

Table I shows the measurement result in detail by giving 10 measured values of fiber size consisting of diameter and height for each array and the mean values are shown in Figure 8. Besides fibers, 5 measurements of cavities for each array are complete and their mean values are shown in Figure 9. Additionally, we repeat the same measurement for fibers on another chip, which is fabricated the same way, and the result is presented in Figure 9. After the mean values of the diameter and height of the fibers in each array on both chip 1 and chip 2 are known, in order to describe the size more accurate, confidence interval is employed.

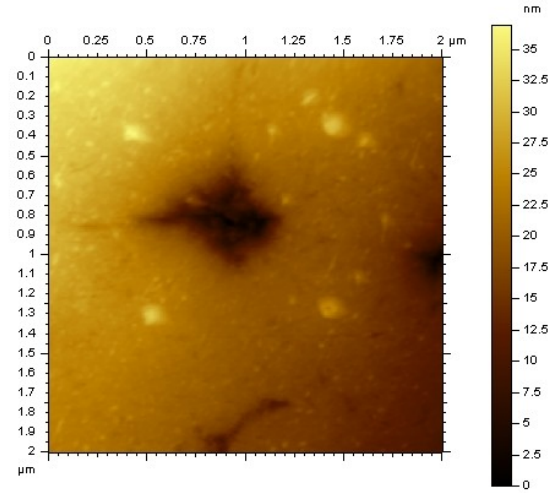

Fig. 5. Zoomed-in topography scan image of array 1 in 2µm square area: both cavity and fiber tip are found.

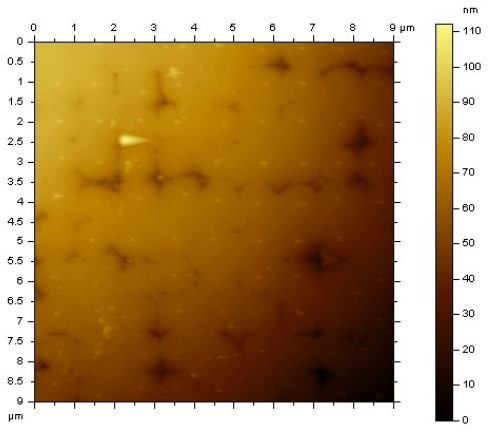

Fig. 4. Topography scan image of array 1 in 9µm square area: cavities are located to zoom in for fibers.

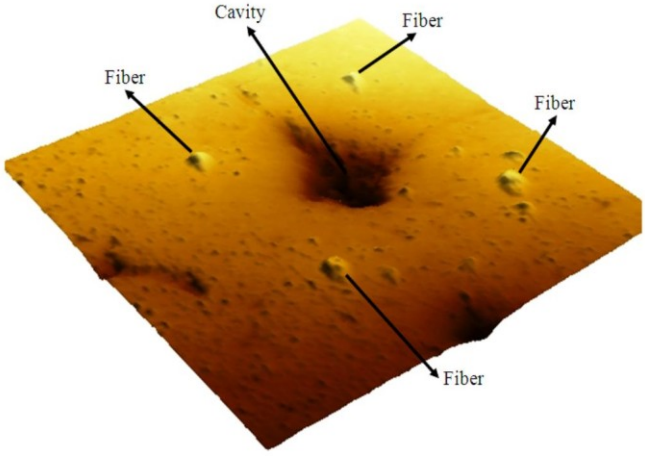

Fig. 6. A 3D image generated based on the 2D topography image as shown in Figure 5.

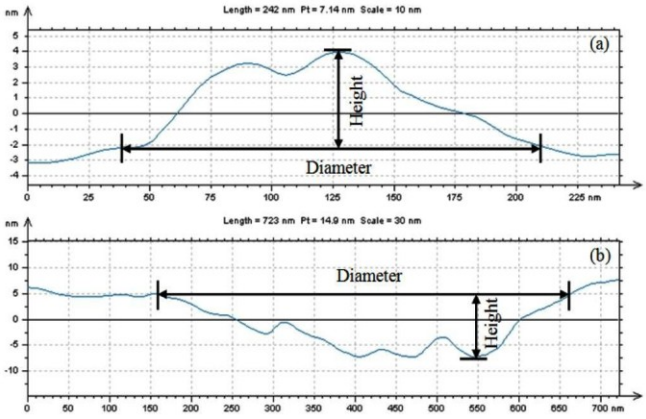

Fig. 7. Cross-section information for measurement based on the line crossing (a) a fiber and (b) a cavity in Figure 6.

TABLE I
RESULT OF MEASUREMENT FOR FIBERS IN CHIP 1

Chip 1	Array 1		Array 2		Array 3	
Meas. #	Diam.	Height	Diam.	Height	Diam.	Height
1	121.43	11	159.64	8.2	164.52	6.8
2	133.18	6.3	139.68	8.1	156.68	5.1
3	129.26	10.7	123.72	6.5	141.01	8.1
4	121.43	5.8	123.72	9.6	164.51	5.4
5	137.1	9.6	137.09	8	152.78	9.1
6	144.93	6	160.6	6.2	133.56	8.4
7	125.34	6.7	148.85	7.7	144.93	10.2
8	148.85	7	156.68	7.5	125.34	10.3
9	137.09	10.2	166.72	9.9	144.99	6.3
10	117.51	6.7	146.34	6.6	117.71	6.4
	Array 4		Array 5		Array 6	
	Diam.	Height	Diam.	Height	Diam.	Height
1	164.53	8.8	144.93	10.9	144.94	7.4
2	168.45	7.6	164.53	8.9	156.75	7.3
3	129.26	6.7	168.44	8.8	148.85	8.4
4	156.68	5.8	160.64	8.4	129.28	8
5	152.53	5.7	161.43	6.1	143.65	6.1
6	155.65	8	153.72	7.5	139.65	7.4
7	163.63	8.2	157.59	7.2	167.59	6.6
8	151.66	6.8	146.06	10	119.72	8.1
9	141.02	9.7	164.54	6.6	152.77	6.8
10	144.93	8.2	148.93	9.3	164.56	6.6
	Array 7		Array 8		Array 9	
	Diam.	Height	Diam.	Height	Diam.	Height
1	135.69	8	139.7	7.6	141.02	7.4
2	143.7	9.1	143.74	7.8	141.02	5.6
3	127.71	6.4	147.67	9.7	129.28	7.1
4	119.75	7.3	151.67	10.9	125.34	7.4
5	121.43	8.2	141.01	9.3	148.85	6
6	117.54	7.8	144.93	7.1	137.12	6.4
7	129.26	6.2	145.04	7.7	133.18	6.6
8	134.29	7.5	133.18	10.2	141.03	6.4
9	117.51	6.4	129.37	7.3	143.69	7.7
10	137.12	5.8	129.35	9.2	135.69	7.2
Overall Mean			**Diameter: 142.87**		**Height: 7.7**	

Remark: all units are in nm.

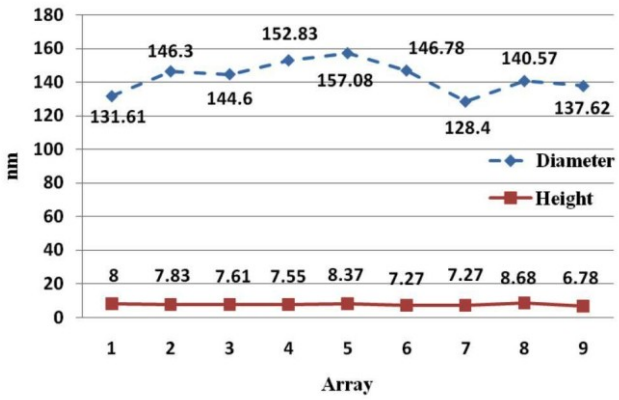

Fig. 8. Measurement result for fiber size in Chip1 presented by the mean values.

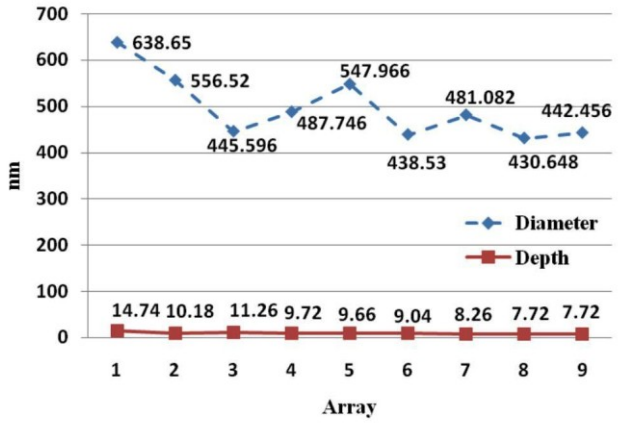

Fig. 9. Measurement result for cavity size in Chip1 presented by the mean values.

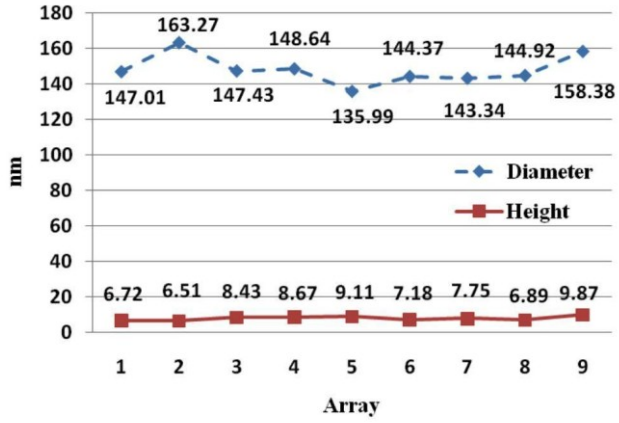

Fig. 10. Measurement result for fiber size in Chip2 presented by the mean values.

B. Statistical Analysis

In statistics, a confidence interval (CI) is an interval estimate of a population parameter. Instead of estimating the parameter by a single value, an interval likely to include the parameter is given. Thus, confidence intervals are used to indicate the reliability of an estimate. How likely the interval is to contain the parameter is determined by the confidence level or confidence coefficient.

Therefore, we apply this statistical method to our

experiment to obtain the interval to describe the size of fibers. Take the fibers in Chip 1 for instance, from Table I and Figure 8, the mean value of 10 measurements for diameter is calculated and we put the value as the first element in a 1×9 matrix. Do the same thing until the matrix is full: {131.61 146.3 144.6 152.83 157.08 146.78 128.4 140.57 137.62}, and then we substitute these samples into the calculation of a 95% confidence interval. The mean of the matrix is 142.87 and the standard deviation is 8.82. Thus, the CI is determined as (137.11; 148.63). For the height, {8 7.83 7.61 7.55 8.37 7.27 7.27 8.68 6.78}, the mean is equal to 7.7 and the standard deviation is 0.554. Thus, the CI can be determined as (7.338; 8.062). Next, based on the data in Figure 9, the standard deviations are 66.65 and 2.07 for cavity diameter and depth respectively. Thus, the 95% CIs can be calculated to describe the diameter and depth. They are (453.03; 540.12) and (8.46; 11.16) respectively. Finally, from Figure 10, another two CIs with same confidence level are computed, (143.13; 153.17) and (7.18; 8.62) for diameter and height respectively. Their standard deviations are 7.68 and 1.11 respectively. Hence, the accurate size of the fibers and cavities can be determined with the intervals as stated.

C. *Result Discussion*

As we can see, some large variations occur to the measurement of the same objective. For example, in Table I Array 2, the fourth measurement of fiber diameter is 123.72nm, which is quite different from the sixth measurement, 160.6nm. Also, we can find the same thing in the measurement of fiber height, like 5.1nm versus 10.3nm in Array 9. This phenomenon is not caused by an incorrect measurement but by the non-uniform growth of the VACNFs on Ni dot nanoelectrodes. The cavities in the arrays will not influence the performance of the nanofibers on the nanoelectrodes as long as the VACNFs growth is not impeded. In the future, since tetraethlyorthosilicate (TEOS) causes the cavities on the surface of the nanoelectrodes, it could essentially be used as a method to create nanochannels for other potential applications such as chemical sensor and pH sensor Lab on Chip System.

V. CONCLUSION

Micro chips with multiplexed 3×3 array biosensor employing patterned VACNFs are ready to work. However, when researchers want to examine the quality of the fabrication, a tool with nano-scale ability is needed. In this paper, the measurement of the VACNFs and the cavities with AFM are carried out and the results presented. As a result, their accurate sizes are indicated statistically by confidence interval.

ACKNOWLEDGMENT

The authors would like to express their sincere gratitude to Prabhu U. Arumugam for chip fabrication at NASA AMES and Holly D. Tourtillot for her help with the experiment. This publication is made possible in part by a grant from the GE Foundation through Michigan State University.

REFERENCES

[1] National Research Council and Committee on Indicators forWaterborne Pathogens, 2004. Indicators for Waterborne Pathogens. National Academies Press, Washington, DC.

[2] K. Dill, D. D. Montgomery, A. L. Ghindilis, K. R. Schwarzkopf, S. R. Ragsdale and A. V. Oleinikov, "Immunoassays based on electrochemical detection using microelectrode arrays : Microarrays for Biodefense and Environmental Applications" 2004. *Biosens. Bioelectron*. 20, 736-742.

[3] O. Niwa and H. Tabei, "Voltammetric Measurements of Reversible and Quasi-Reversible Redox Species Using Carbon Film Based Interdigitated Array Microelectrode", 1994. *Anal. Chem.* 66(2), 285-289.

[4] J. Li, J. Koehne, A. M. Cassell, H. Chen, Q. Ye, H. T. Ng, J. Han and M. Meyyappan, "Miniaturized Multiplex Label-Free Electronic Chip for Rapid Nucleic Acid Analysis Based on Carbon Nanotube Nanoelectrode Arrays", 2004a. *J. Mater. Chem.* 14, 676-684.

[5] J. Li, J. Koehne, A. M. Cassell, H. Chen, Q. Ye, H. T. Ng, J. Han and M. Meyyappan, "Bio-Nano Fusion in Sensor and Device Development", 2004b. *MCB 1* (1), 69-80.

[6] M. A. Guillorn, T. E. McKnight, A. Melechko, V. I. Merkulov, P. F. Britt, D. W. Austin, D. H. Lowndes and M. L. Simpson, "Individually Addressable Vertically Aligned Carbon Nanofiber Based Electrochemical Probes", 2002. *J. Appl. Phys.* 91 (6), 3824-3828.

[7] P. He and L. Dai, "Aligned Carbon Nanotube-DNA electrochemical Sensors", 2004. *Chem. Commun.*, 348-349.

[8] Y. H. Yun, V. Shanov, M. J. Schulz, Z. Dong, A. Jazieh, W. R. Heineman, H. B. Halsall, D. K. Y. Wong, A. Bange, Y. Tuf and S. Subramaniam, "High Sensitivity Carbon Nanotube Tower Electrodes", 2006. *Sens. Actuators B 120*, 298-304.

[9] P. V. Gerwen, W. Laureyn, W. Laureys, G. Huyberechts, M. O. D. Beeck, K. Baert, J. Suls, W. Sansen, P. Jacobs, L. Hermans and R. Mertens, "Nanoscaled Interdigitated Electrode Arrays for Biochemical Sensors", 1998. *Sensors and Actuators B*, vol. 49, 73-80.

[10] F. Patolsky, G. Zheng and C. M. Lieber, 2006. "Fabrication of Silicon Nanowire Devices for Ultrasensitive, Label-Free, Real-Time Detection of Biological and Chemical Species", *Nat. Protocols 1*, 1711-1724.

[11] N. Yang, H. Uetsuka, E. Osawa and C. E. Nebel, "Vertically Aligned Diamond Nanowires for DNA Sensing", 2008. *Angew. Chem. Int. Ed. 47*, 5183-5185.

[12] J. Li and M. Meyyappan, 2004. Carbon Nanotubes: Science and Applications. CRC Press, Boca Raton, FL.

[13] A. V. Melechko, V. I. Merkulov, T. E. McKnight, M. A. Guillorn, K. L. Klein, D. H. Lowndes and M. L. Simpson, 2003. "Large-Scale Synthesis of Arrays of High-Aspect-Ratio Rigid Vertically Aligned Carbon Nanofibers". *Nanotechnology* 14(2003), 1029-1035.

[14] Prabhu U. Arumugam, Hua Chen, Shabnam Siddiqui, Jarret A. P. Weinrich, Ayodeji Jejelowo, Jun Li and M. Meyyappan, "Wafer-Scale Fabrication of Patterned Carbon Nanofiber Nanoelectrode Arrays: A Route for Development of Multiplexed, Ultrasensitive Disposable Biosensors", *Biosensors and Bioelectronics*, 24(2009), 2818-2824.